American Mineralogist, Volume 96, pages 1748–1759, 2011

In-situ mid/far micro-FTIR spectroscopy to trace pressure-induced phase transitions in strontium feldspar and wadsleyite

Maria Mrosko,[1,*] Monika Koch-Müller,[1] and Ulrich Schade[2]

[1]Helmholtz-Zentrum Potsdam, Deutsches GeoForschungsZentrum-GFZ, Telegrafenberg, 14473 Potsdam, Germany
[2]Helmholtz-Zentrum Berlin für Materialien und Energie, Albert-Einstein-Strasse 15, 12489 Berlin, Germany

Abstract

As representatives of nominally anhydrous minerals (NAMs) in the crust and mantle the pressure-dependent behavior of strontium feldspar and wadsleyite, containing different amounts of water, was studied in a diamond-anvil cell via mid and far IR spectroscopy up to 24 GPa. The samples were synthesized in a piston-cylinder press at 2 GPa/700 °C (strontium feldspar) and in a multi-anvil apparatus at 13.8 GPa/1000 °C (dry wadsleyite) and 13.2 GPa/1150 °C (hydrous wadsleyite). The water content of the samples was determined by polarized FTIR and Raman spectroscopy. The strontium feldspar crystals (up to 300 μm) contained about 1100(100) wt ppm water. The hydrous wadsleyite crystals (up to 240 μm) contained 12 500(900) wt ppm water. The synthesis of dry wadsleyite yielded a fine-grained powder. A new THz/FIR-microscope for the synchrotron source BESSY was developed to conduct the diamond-anvil cell measurements in the far IR region. Conventional in-situ mid IR spectroscopy was also performed on all samples. The measurements on strontium feldspar showed a phase transformation at 6.5(5) GPa (space group $I2/c$ to $P2_1/c$). The wadsleyite analyses revealed a phase transition at approximately 8.4(7) GPa in the hydrous and approximately 10.0(7) GPa in the dry sample. It probably represents a transition from an orthorhombic to a monoclinic structure. The high amount of water incorporated in the hydrous wadsleyite shifts the transformation toward lower pressures compared to the dry one. By comparison, the relatively low amount of water in strontium feldspar does not change the stability relations compared to the dry one. Therefore, water incorporation in nominally anhydrous minerals may have an effect on the pressure of phase transitions, whereas the extent of that influence strongly depends on the structure of the phase and the amount of water carried within the mineral.

Keywords: Wadsleyite, strontium feldspar, mid/far FTIR spectroscopy, phase transition, water

Introduction

Infrared spectroscopy generally is a very sensitive probe for information on the local microscopic structure and bonding in minerals. When combined with a high brightness synchrotron source, infrared microspectroscopy offers the opportunity to achieve the spatial resolution approaching the diffraction limit of light. It enables us to investigate pressure-induced structural changes in the THz/FIR (far infrared) region of geomaterials placed in diamond-anvil cells (DAC) up to 30 GPa. In the mid-infrared range (MIR), vibrations of the more rigid $Si(Al)O_4$-tetrahedra are predominantly found, whereas measurements in the far infrared yield information on metal cation motion. By tracing these vibrations as a function of pressure, important information on the nature of a possible phase transition may be deduced. We applied this methodology to study the response of strontium feldspar (an analog for anorthite as representative of the crust) and wadsleyite (as representative of the mantle) structures to changes in pressure. Both minerals are nominally anhydrous but can incorporate hydrogen in the form of hydroxyl groups via point defects in their structures in trace amounts in strontium feldspar (Mrosko et al. 2010) and up to several weight percent in wadsleyite (Deon et al. 2010a). Both structures are very susceptible to changes in pressure and several pressure-induced phase transitions have been reported (Chopelas 1991; Cynn and Hofmeister 1994; McGuinn and Redfern 1994; Pandolfo et al. in review). It is known that even small amounts of water in nominally anhydrous minerals may change their rheological, structural, and thermodynamic properties (e.g., Smyth and Kawamoto 1997). However, up to now it is not clear whether the incorporated hydrogen has an influence on the pressure range where these transitions occur. Jacobsen et al. (2010) demonstrated that incorporation of 1300 ppm H_2O (as OH^-) in $MgSiO_3$ displaces the transition of low- to high-pressure clinoenstatite by up to 2 GPa toward lower pressure. Furthermore, Deon et al. (2010b) observed a shift of the transformation pressure of olivine to wadsleyite in the system MgO-SiO_2-H_2O of about 0.6 GPa to lower pressures due to higher water fractionation into wadsleyite (8000 wt ppm) compared to olivine (2000 wt ppm).

To study the effect of water on phase stabilities, well-developed single crystals with accurately defined water concentrations are needed. Anorthite belongs to the group of feldspar minerals,

* E-mail: mrosko@gfz-potsdam.de

0003-004X/11/1112–1748$05.00/DOI: 10.2138/am.2011.3731

which represents the most common silicate within the Earth's crust. The synthesis conditions of OH-bearing anorthite single crystals are limited to low pressures as anorthite transforms to zoisite (plus kyanite and quartz) at 1 GPa and 700 °C in the presence of water. However, low-pressure syntheses solely consist of white powders with crystal sizes not exceeding 10 μm (Mrosko et al. 2010), which impedes a precise quantification of the water content. Strontium feldspar is often used as analog material for anorthite as high-pressure syntheses in the presence of water yield well-defined idiomorphic crystals (Mrosko et al. 2010). At ambient conditions, the strontium end-member crystallizes with monoclinic symmetry with space group $I2/c$. The transition to the triclinic structure along the calcium-strontium-anorthite join was determined for compositions close to An_9SrF_{91} (McGuinn and Redfern 1994). These authors also found a pressure-driven ferroelastic phase transition at 3.2(0.4) GPa in pure strontium feldspar from space group $I2/c$ to $I\bar{1}$. Pandolfo et al. (in review) reported a first-order phase transition at 6.6 GPa from space group $I2/c$ to $P2_1/c$ for both a dry and synthetic OH-bearing strontium feldspar described in Mrosko et al. (2010) that was also used in this study.

The three $(Mg,Fe)_2SiO_4$ polymorphs olivine (α), wadsleyite (β), and ringwoodite (γ; with increasing pressure) are the main constituents of the Earth's upper mantle and transition zone. Investigations of these polymorphs reveal important insights, e.g., about phase relations and water storage in the Earth's mantle. Wadsleyite is a nominally anhydrous mineral; nevertheless, it has already been shown that it can incorporate water up to 3.3 wt% H_2O in its structure via point defects (e.g., Inoue et al. 1995). With such high amounts of incorporated hydrogen, orthorhombic wadsleyite, on the one hand, can transform to monoclinic symmetry (Smyth et al. 1997; Tsuchiya and Tsuchiya 2009). On the other hand, additional phases in the system of hydrous magnesium silicates, such as wadsleyite II, can be found. Wadsleyite II incorporates 2.0–2.7 wt% H_2O and was synthesized by Smyth and Kawamoto (1997) in experiments containing a multi-component mantle composition. The structure of wadsleyite II is quite similar to wadsleyite with orthorhombic symmetry and space group *Imma* but has a *b* dimension that is 2.5 times longer. The vibrational behavior of wadsleyite has been examined in several studies, both experimentally and via computational modeling (Chopelas 1991; Cynn and Hofmeister 1994; Wu and Wentzcovitch 2007). Pressure-dependent studies revealed evidence for a second-order structural phase transition around 9 GPa (Chopelas 1991; Cynn and Hofmeister 1994) in wadsleyite, although of different compositions (magnesium end-member, no water reported, and iron-bearing with 0.2 wt% H_2O, respectively).

Measurements in the far IR region could help to clarify the nature of the phase transition. These kinds of measurements are still rare, especially since the study of the pressure-dependence of FIR vibrations reveals some difficulties, such as the weakness of the absorption bands (Cynn and Hofmeister 1994) and the loss of intensity of radiation when approaching the diffraction limit of light at longer wavelengths. In contrast, pressure-dependent Fourier transform infrared (FTIR) spectroscopy in the mid IR region is easy to conduct and offers the ability to trace phase transitions especially for lower symmetry phases with many bands. The combination of synchrotron FIR measurements and conventional MIR spectroscopy in this study provides a broad overview of structural changes in a wide spectral range.

We applied in situ high-pressure FTIR spectroscopy in both the mid and far IR region to hydrous strontium feldspar and dry and hydrous wadsleyite from 2000 down to 30 cm^{-1}. We show that phase transitions and their potential nature can be more clearly traced by combining both conventional and synchrotron techniques, and that water incorporation can have an effect on the pressure range of these transitions.

Experimental and analytical methods

Syntheses

Strontium feldspar–piston-cylinder press. The strontium feldspar was synthesized in a non-endloaded piston-cylinder press at 2 GPa and 700 °C. Further details of the experimental conditions as well as structural and chemical investigations are specified in Mrosko et al. (2010) and are summarized in Table 1.

Wadsleyite–multi-anvil press. The high-pressure syntheses of wadsleyite were performed in a multi-anvil apparatus similar to that of Walker (1991) but with a special tool, which allows alternatively a continuous 360° rotation or a 180° rocking motion of the Walker high-pressure module during the run with 5°/s to avoid separation of the fluid from the solid parts of the run and thus ensure a homogenous starting material (see Schmidt and Ulmer 2004; Deon et al. 2010a). We used a 14/8-assembly (octahedron length/truncation length) with an MgO-based octahedron serving as a pressure-transmitting part, a stepped graphite heater, and pyrophyllite gaskets. The temperature was controlled by a W5%Re-W26%Re thermocouple. Details of the experimental setup are given in Koch-Müller et al. (2009).

An afore synthesized forsterite powder (pressed disks of a ground $2MgO\text{-}SiO_2$ mixture, left for 5 days at 1300 °C, ground, and pressed again after two days) served as starting material for the dry synthesis and was filled into Pt capsules (length 3 mm, outer diameter 2 mm). For the hydrous runs an amount of 0.5 mg (5 wt%) distilled water was first filled into the capsule before adding the starting material. The filled capsule was then cold-sealed. Final values for pressure and temperature were 13.8 GPa/1000 °C (dry) and 13.2 GPa/1150 °C (hydrous). After 20 h (dry run) and 8 h (hydrous run), we quenched the experiments and checked the hydrous run for the presence of excess water.

Analyses

X-ray diffraction. Powder X-ray diffraction (XRD) measurements on all samples were done in transmission mode with a STOE Stadi P diffractometer, equipped with a curved Ge (111) primary monochromator, a 7° wide position sensitive detector (PSD), and Cu$K\alpha$-radiation. Unit-cell dimensions were determined using the GSAS software package for Rietveld refinement (Larson and Von Dreele 2000). Initial structures for refinement derive from Chiari et al. (1975) for strontium feldspar and Finger et al. (1993) for wadsleyite.

Raman spectroscopy. The Raman spectra were taken to quantify the water content in wadsleyite using a Horiba Jobin Yvon Labram HR 800 UV-VIS spectrometer in a backscattering configuration equipped with an argon laser, a CCD detector and an Olympus optical microscope with a long working distance 100× objective and a confocal optic with a 100 μm pinhole. The Raman scattering was excited by the blue line of the argon laser (488 nm) working at 300 mW. We applied the Comparator technique for water quantification (Thomas et al. 2008, 2009). For this purpose, crystallographically oriented single crystals of hydrous wadsleyite (MA207) were embedded into an epoxy-matrix and polished one-sided. The focal point of the laser beam was adjusted approximately 4 μm beneath the polished sample surface to reduce artifacts due to surface effects. Each sample was measured twice—with E parallel to the particular optical indicatrix axes. A glass with known water content of 8.06 wt% was used as a reference for all measurements and its Raman spectrum was measured before and after the sample measurements. Counting times were 100 s on the standard (2400–4000 cm^{-1}) and on the sample (3000–3800 cm^{-1}), with threefold accumulation. The water concentration in moles per liter was calculated using the formula:

$$c_{H_2O} = I_{corwad} \times \frac{c_{H_2O\_ref}}{I_{ref}}$$

TABLE 1. Experimental conditions and results

Sample	Experimental conditions and phase fraction in wt%	Space group EMPA	Lattice constants*	Water content (wt ppm)
Sr-anorthite (SrAn2)	2 GPa/700 °C ~QFM 90% Sr-anorthite 3% strontianite 7% slawsonite	Monoclinic space group *I2/c*† ‡ $Sr_{1.005(6)}Al_{1.995(8)}Si_{2.000(8)}O_8$	*a* (Å) = 8.3970(3) *b* (Å) = 12.9714(5) *c* (Å) = 14.2557(4) β (°) = 115.490(4)	440(40)
Sr-anorthite (SrAn1)	2 GPa/700 °C Fe-FeO 100% anorthite	Monoclinic space group *I2/c* $Sr_{0.962(17)}Al_{1.991(10)}Si_{2.025(14)}O_8$	*a* (Å) = 8.3956(9) *b* (Å) = 12.976(2) *c* (Å) = 14.264(1) β (°) = 115.501(6)	320(30)
Hydrous wadsleyite (MA207)	13.2 GPa/1150 °C	Orthorhombic space group *Imma*	*a* (Å) = 5.6798(12) *b* (Å) = 11.5462(23) *c* (Å) = 8.2518(15)	12500(900)
Dry wadsleyite (MA234)	13.78 GPa/1100 °C	Orthorhombic space group *Imma*	*a* (Å) = 5.6991(14) *b* (Å) = 11.4426(28) *c* (Å) = 8.2560(18)	

* 2σ standard deviation.

† $R(p) = \sum_i \left| Y_{i,\mathrm{obs}} - Y_{i,\mathrm{calc}} \right| / \sum_i Y_{i,\mathrm{obs}} = 5.4\%$

‡ DWd: serial correlation after Durbin and Watson, see Post and Bish (1989) = 1.6.

where I_{ref} is the intensity of the reference (summed up over the three identical directions in the reference glass) and I_{corwad} is the corrected intensity of the sample determined by:

$$I_{\mathrm{corwad}} = \sum I_{\mathrm{wad}} \times c_{V\_\mathrm{wad}} \times \frac{100}{c_{R\_\mathrm{wad}}}.$$

ΣI_{wad} refers to the sum of the total integrated intensities measured in the three crystallographic directions and c_{R_wad} refers to a correction factor (accounting for the difference of the reflectivities) calculated for wadsleyite as 94.3. The correction factor c_{V_wad} accounts for the different sampling volume in wadsleyite compared to the reference glass. Thomas et al. (2008, 2009) suggested using the density ratio $\rho_{\mathrm{glass}}/\rho_{\mathrm{wad}}$ as a correction; however, in the case of minerals with heavy metal cations, this approach is not correct, and we propose here a more general correction factor:

$$c_{V\_\mathrm{sample}} = \frac{\frac{V_{M\_\mathrm{sample}}}{n_{\mathrm{atoms(pfu)\_sample}}}}{\frac{V_{M\_\mathrm{reference}}}{n_{\mathrm{atoms(pfu)\_reference}}}}.$$

Since glass is very close to tridymite in terms of its structural properties, we took the molar volume of tridymite $V_{M\_\mathrm{reference}}$ from a database as 25.54 $\mathrm{cm^3/mol}$ and calculated with 3 atoms per formula unit (apfu). The molar volume of wadsleyite V_{M_sample} was calculated as 40.79 $\mathrm{cm^3/mol}$ with 7 apfu. The resulting c_{V_wad} was then estimated as 0.684. For the Mg_2SiO_4 polymorphs, the density correction proposed by Thomas et al. (2009) would give the same result.

FTIR spectroscopy. The pressure-dependent MIR-measurements were performed at GFZ using a Bruker IFS 66/v FTIR spectrometer and an attached Hyperion microscope. A globar served as light source. Additional devices were an MCT detector and a KBr beam splitter. The spectra were collected on thin films of the sample placed in a diamond-anvil cell (see below) with a resolution of 2 $\mathrm{cm^{-1}}$. The spectra were averaged over at least 256 scans over the range of 4000(1800) to 400 $\mathrm{cm^{-1}}$. The background was measured through the same cell.

IR spectroscopy in the longer wavelength range (FIR) with diamond-anvil cells using apertures of about 0.3 mm to reach high pressures brings up some difficulties as with increasing radiation wavelength intensity is lost due to diffraction of the light. Hofmeister et al. (1989) were the first who applied far IR spectroscopy in combination with diamond-anvil cell experiments up to 43 GPa using a laboratory light source. Due to the loss of intensity through the small aperture radius (gasket hole) needed for high pressures, the measurement time of one spectrum was about one hour. An additional problem encountered was atmospheric water vapor, which also results in loss of intensity and in a multitude of IR bands that occur in the far IR range. High-quality IR spectra measured within a reasonable time span can be obtained by using synchrotron radiation. Synchrotron IR radiation has the same diffraction limitation but due to its high brilliance enough intensity is maintained for the measurements. The FIR microspectroscopy was done at the Helmholtz-Zentrum Berlin, BESSY II at the Synchrotron IR beamline IRIS (Peatman and Schade 2001). For this purpose, we developed a THz/FIR microscope adapted to a Bruker IFS 66/v FTIR spectrometer, which allows measurements under vacuum down to the THz region. The combination of high brilliance synchrotron light and the new microscope working under vacuum enabled us to take a spectrum with a very good signal-to-noise ratio within a few minutes and even covered a larger spectral range compared to the study of Hofmeister et al. (1989). Figure 1 shows the microscope with all relevant devices mounted on a ground plate (250 × 250 mm). The whole construction is easily set into the sample compartment of the spectrometer. The cell itself is screwed into a holder and is therefore adjustable from the outside by the x- and y-screws even under vacuum. After passing a 6 µm biaxially-oriented polyethylene terephthalate (BoPET) broadband beam splitter, the incident IR-synchrotron light is directed into the sample compartment and through several mirrors focused by the cassegrain objective (NA = 0.28) directly into the sample chamber of the diamond-anvil cell. After passing through the cell, the transmitted light is directed through another arrangement of mirrors to the LHe-cooled bolometer (detector). With this device, we were able to collect FIR spectra up to 24 GPa. No additional aperture, other than the gasket hole itself, was used during the measurements. See Table 2 for further details concerning the IR spectroscopy.

For both the mid and far IR measurements, single crystals of strontium feldspar and hydrous wadsleyite were pressed into thin films by using a diamond-anvil cell without a gasket. Due to the strong absorbance, the film for the MIR measurements was about 5 µm thick, although for the weaker FIR modes a film of about 30–50 µm was needed. In the case of dry wadsleyite, small amounts of powder were pressed into films. Afterward, the thin films were loaded into a Mao-type diamond-anvil cell with type II diamonds with a culet size of 400 to 600 µm and preindented stainless steel gaskets with 300–450 µm holes and a thickness of approximate 0.3 mm. In the case of the FIR measurements, the film was aimed to cover as much of the gasket hole as possible. The thin film, a few small ruby crystals (strontium feldspar) and ruby spheres (wadsleyite), respectively, and the pressure-transmitting medium (either argon, neon, CsI, or petroleum jelly) were loaded into the sample chamber. We performed the measurements in transmission mode whereas the background spectrum was taken through a separate cell (empty or filled with the particular pressure-transmitting medium). Afterward, we calculated the final absorbance spectrum by applying the following procedure:

$$A = \lg\left[\left(\frac{I_{\mathrm{sample}}}{I_{\mathrm{empty\ light\ path\_sample}}} \Big/ \frac{I_{\mathrm{background\ cell}}}{I_{\mathrm{empty\ light\ path\_bg}}}\right)^{-1}\right]$$

Due to multiple reflections between plane-parallel surfaces (diamond culets) or within thin layers (sample), we were faced with the phenomenon of interference fringes that covered the IR spectra. In these cases we applied the procedure proposed by Neri et al. (1987) to remove the interferences by shifting the measured spectrum $G(x_n)$ half wavelength ($d/2$) of the interference maxima up and down (with $2m$ being the number of points within the interference period d), respectively, and combining the three curves as follows:

$$F(x_n) = \frac{1}{4}\left[2G(x_n) + G(x_{n+m}) + G(x_{n-m})\right].$$

We used different pressure-transmitting media to see if there is a difference in the pressure behavior of the minerals. The simplest pressure media to load are petroleum jelly (used only in the FIR) and CsI (used in the MIR). Argon was loaded cryogenically, but as described by Wittlinger et al. (1997) it undergoes a structural reorganization around 9 GPa, which potentially has an effect on the pressure-dependent behavior of the sample (see Koch-Müller et al. 2010). Although heating of the whole cell up to 120 °C antagonizes the structural modification of argon (hereinafter referred to as annealed argon), we proceeded to use neon as a pressure-transmitting medium. The high compressibility of neon induces, however, a shrinking of the gasket hole up to 30% during the loading procedure. The initial gasket hole was chosen in such a way that the final diameter was at least 200 µm. We aimed to set the size of the film so that it finally covered the gasket hole without being squeezed, although Hofmeister et al. (1989) showed that a probable squeezing of the sample (in the case of forsterite) does not affect the IR spectra.

The pressure was determined by measuring the R2-fluorescence line of ruby after each pressure increase by applying the calibration of Mao et al. (1986). The stated value represents the average of determined pressures before and after the IR measurements.

Autocorrelation analysis. The autocorrelation analysis is a mathematical approach to reveal the effective line width of absorption bands or groups of bands in IR spectra. In this way, continuous changes in the behavior of these bands due to structural or chemical variations can be quantitatively described by a general state parameter Q. To perform the autocorrelation analysis we followed the concept and procedure described by Salje et al. (2000). These authors stated that by applying density functional perturbation theory one can consider Q as the state variable, which is then associated directly with the integrated intensity I, the frequency ω, and the line width γ of the spectra. For this purpose, one has to select a certain range within the phonon spectrum containing one or more bands with the endpoints lying on a linear baseline. The chosen segment is then correlated with itself by means of the autocorrelation function:

$$Corr(\alpha,\omega') = \int_{-\infty}^{\infty} \alpha(\omega+\omega')\alpha(\omega)\,d\omega$$

where α(ω) is the original spectrum, which is offset by a range of successive frequencies ω′. The width $k2$ of the central peak of the resultant autocorrelation spectrum at $\omega \rightarrow 0$ contains quantitative information about the bands' line width in the primary spectrum. Therefore a Gaussian curve is fitted to the central peak of every (ω′—shifted) autocorrelation spectrum and the resultant $k2$-values are plotted against the frequency shift ω′. Due to noise in the original spectrum $k2 \rightarrow 0$, labeled as Δ*corr*, is determined, not directly, but by means of extrapolation by applying a polynomial function. Discontinuities in the slope of Δ*corr* with increasing pressure indicate sudden changes in the line width of the band group in the original spectrum and can be assigned to possible phase transitions.

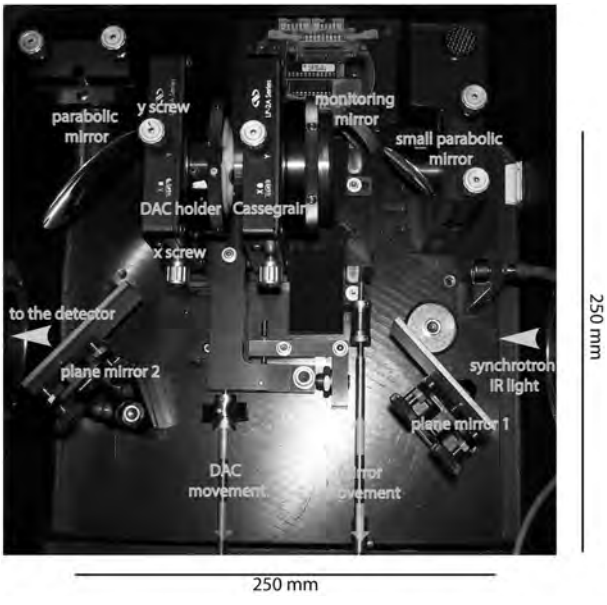

Figure 1. Picture of the far IR microscope set into the sample compartment of the spectrometer (BRUKER IFS 66/v operating under vacuum) at BESSY.

Results

Strontium feldspar

Structural-chemical analyses. The piston-cylinder experiments yielded optically clear single crystals of 50–300 µm in size with idiomorphic as well as anhedral morphology. These crystals were characterized by electron microprobe analyses (EMPA), powder XRD and IR spectroscopy for the OH-content by Mrosko et al. (2010). The OH^- concentration (expressed in the following discussion as wt ppm H_2O) was about 440(40) wt ppm when we only considered structural OH^- and about 1100(100) wt ppm when we included the contribution of molecular H_2O, either structurally bonded or in microinclusions (Mrosko et al. 2010). The data are summarized in Table 1.

IR spectroscopy at ambient conditions. Figure 2 displays a merge of an ambient mid and far IR spectrum of strontium feldspar. We followed the band assignment of Iiishi et al. (1971) for the entire spectral range.

The mid-infrared part shows the most intense bands between 1200 and 800 cm^{-1}. These modes are assigned to stretching vibrations of Si-O (1078 cm^{-1}) and Si-(Al)-O (1033, 958 cm^{-1}). That part is followed by two sequences of much weaker but clearly defined bands at 800–650 and 650–400 cm^{-1}. The first section again contains modes of stretching vibrations of Si-Si (753 cm^{-1}), Si-Al(Si) (725 cm^{-1}) and Al(Si)-O (at 684 and 673 cm^{-1}). The second section is mostly characterized by bending vibrations of O-Si(Al)-O (625, 605, 576 cm^{-1}) and a few combination modes of O-Si-O bending plus Sr-O stretching vibrations. Subsequently one finds two Si-O-Si bending modes (397 and 389 cm^{-1}). In

Table 2. Parameters of pressure-dependent FTIR spectroscopy

Sample	Range (cm^{-1})	No. of scans	Resolution (cm^{-1})	Aperture (µm × µm)	Beamsplitter	Detector	Pressure-transmitting medium
Sr-anorthite	1800–400	256	2	~80 × 60	KBr	MCT	Annealed Ar/CsI
Sr-anorthite	800–50	1024	4	300 × 300	Broadband BoPET 6 µm	Bolometer	Annealed Ar
Hydrous wadsleyite	4000–400	512	2	55 × 55	KBr	MCT	Ne
Hydrous wadsleyite	700–20	128/256	4	200 × 200/ 300 × 300	Broadband BoPET 6 µm	Bolometer	Ne/petroleum jelly
Dry wadsleyite	4000–400	1024	2	80 × 100	KBr	MCT	Ne
Dry wadsleyite	700–20	256	4	300 × 300	Broadband BoPET 6 µm	Bolometer	Petroleum jelly

the adjacent far IR region, one observes almost all bands being weaker and less characteristic. The strongest bands in that range are located at 373, 346, 296 cm^{-1} [Si-O-Si(Al) deformation and torsional vibrations] and at 228, 180, 157, 123, and 93 cm^{-1} (all are Sr-O stretching vibrations).

Pressure-dependent mid and far IR spectroscopy. The pressure-dependent measurements in the DAC shown in Figures 3 (MIR) and 4 (FIR) display a general trend for all bands, which is a shift toward higher wavenumbers and a broadening with increasing pressure.

As visualized by the straight lines in Figure 3, the pressure-induced shifts of the MIR bands at 1033, 753, and 725 cm^{-1} are constant up to 6.8(5) GPa. The next pressure step to 7.7(5) GPa results in a clear jump back of the band maxima in conjunction with strong broadening and the evolution of a new band seen as a shoulder around 940 cm^{-1} (circle) that persists through a further increase of pressure.

Another discontinuity—though less obvious than the last described—is present between 10.1(5) and 11.8(5) GPa and is characterized by an even stronger broadening of the bands that may be due to overlap. Furthermore one observes the development of another shoulder at 920 cm^{-1} (circle) as well as a strong smearing of the bands around 600 cm^{-1}.

The positions of the far IR bands as a function of pressure are shown for three bands in Figure 5. The wavenumbers of the selected bands at ambient conditions are 296, 228, and 180 cm^{-1}. The dashed lines indicate the slope changes of the pressure-dependent wavenumber shifts that are located at approximately 6.5(5) and in a broad range around 12.0(5) GPa. The corresponding values for dv/dP (in cm^{-1}/GPa) calculated by linear regression of the data from ambient to 6.5(5) GPa and from 6.5(5) to 12.0(5) GPa (solely the data on pressure increase were used) are 0.07 and 1.38 (296 cm^{-1}), 1.14 and 5.23 (228 cm^{-1}), and 1.6 and 0.3 (180 cm^{-1}), respectively. No autocorrelation analysis was performed on these data sets, as the pressure-induced changes were obvious by eye-inspection.

Wadsleyite

Structural-chemical analyses. The synthesis of dry wadsleyite yielded a very fine-grained single-phase powder with small crystals in orthorhombic symmetry (space group *Imma*). In the case of hydrous wadsleyite, we were able to produce clear single crystals ranging from 50–240 µm in size. X-ray diffraction analyses also revealed orthorhombic symmetry and space group *Imma*. Water quantification yielded 12 500(900) wt ppm water. For further details see Table 1.

IR spectroscopy at ambient conditions. Figures 6 and 7 display spectra of wadsleyite at ambient conditions. Figure 6 depicts a merged FIR and MIR spectrum of dry wadsleyite. It shows clearly that bands in the mid IR region are stronger than those in the FIR region. Figure 7 compares the mid IR spectra of dry and hydrous wadsleyite (12 500 wt ppm H_2O).

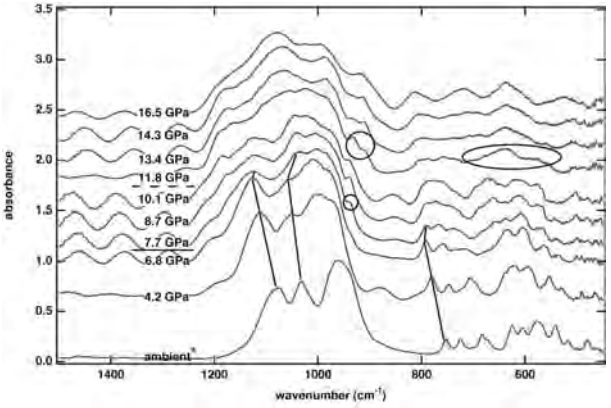

FIGURE 3. Pressure-dependent MIR absorption spectra of strontium feldspar (pressure-transmitting medium: annealed argon). The spectrum at ambient conditions (*) was yielded after decompression. The black lines and circles serve as a guide to point out the changes. Spectra are offset for clarity.

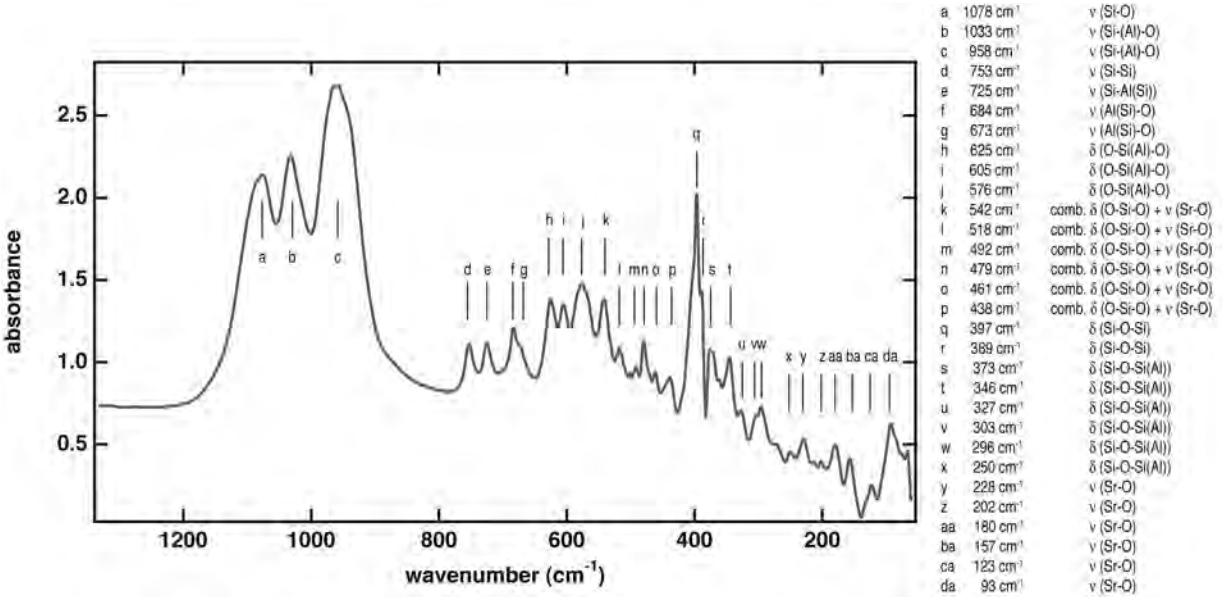

FIGURE 2. Merged absorption spectrum (MIR and FIR) of strontium feldspar with band assignments after Iiishi et al. (1971).

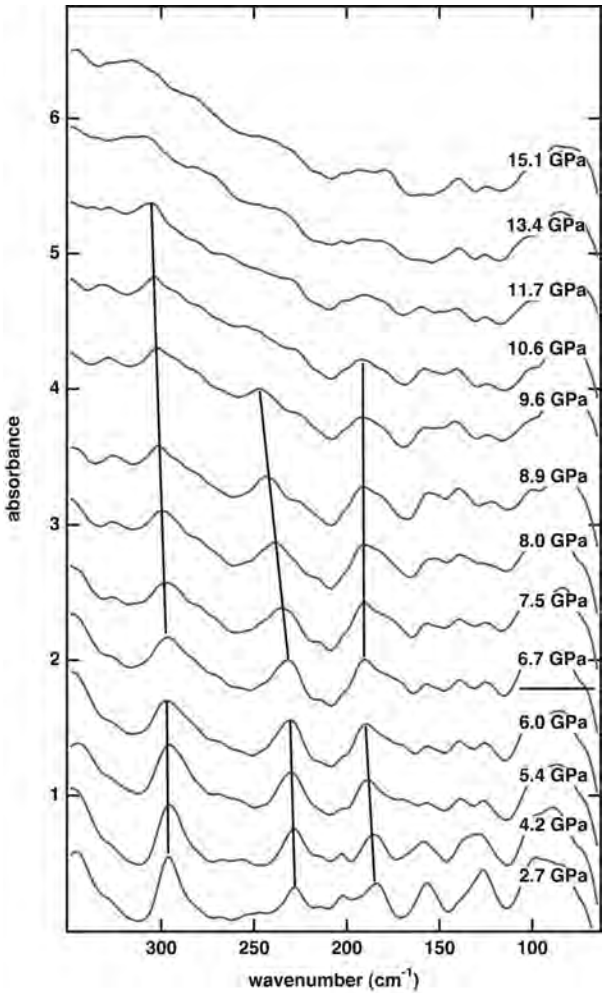

FIGURE 4. Pressure-dependent FIR absorption spectra of strontium feldspar (pressure-transmitting medium: annealed argon). The black lines display the development of three bands. Spectra are offset for clarity.

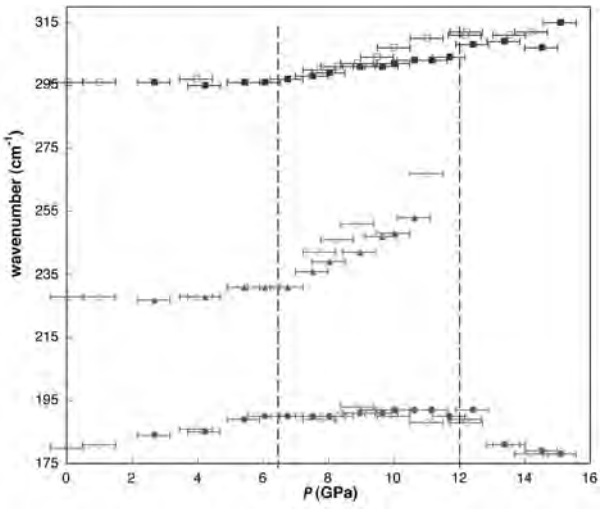

FIGURE 5. Pressure vs. wavenumber plot of three FIR bands in strontium feldspar. The filled symbols correspond to values yielded upon pressure increase; the open symbols represent the data at decreasing pressure. The dashed lines mark the locations of changing slopes. The first slope change at about 6.5 GPa is quite clear and visible in all three bands. The second slope change around 11 GPa, however, is less obvious. Error bars: 0.5 GPa in pressure (from averaged measurements before and after the spectra were taken) and within the symbol in wavenumber-direction.

The classification of all bands follows those reported in Cynn and Hofmeister (1994), whereas the assignments of Wu and Wentzcovitch (2007) derived from a density functional study will be integrated in a later discussion.

The most intense group in the spectrum of wadsleyite lies between 1100 and 750 cm^{-1} and is due to asymmetric [937, shoulder at 918 cm^{-1} (dry), 944 and shoulder at 915 cm^{-1} (hydrous)] and symmetric (812 or 805 cm^{-1}) stretching vibrations of SiO_3 followed by the weaker ν_s(Si-O-Si) at 701 cm^{-1}. The mode of the asymmetric deformation band $\rho(Si_2O_7)$ is assigned to the band at 599 cm^{-1}. It is of medium intensity, whereas the following stretching vibration bands are characterized as (M3-O1) and display weaker (550, 535, 519, and 422 cm^{-1}) or quite high (487 cm^{-1}) intensity (dry sample). The spectrum of the hydrous wadsleyite is very similar to the dry one, however, it shows for the Si-O stretching vibrations significant higher full-width at half maximum (FWHM). In addition to the higher FWHM, the most striking difference compared to the spectrum of the dry sample is the occurrence of additional bands around 682 and 573 cm^{-1}, whereas the dry-wadsleyite-band at 550 cm^{-1} seems to be completely missing. In addition, the intensity of the band at 599 cm^{-1} decreases significantly with water incorporation. These features are distinctive and we observed them also in other wadsleyite samples.

The translational mode T(M) at 361 cm^{-1} is the most intense one, followed by two overlapping bands of the same kind at ~318 and 294 cm^{-1}. Subsequently, one can distinguish three or four very weak and asymmetric (flat-lying) bands at 260 cm^{-1} (rotational), 212 cm^{-1} (small shoulder at 190 cm^{-1}, both translational vibrations), and one around 144 cm^{-1} that is likely to be a rotational mode.

Pressure-dependent mid and far IR spectroscopy. Figures 8a and 8b (dry and hydrous wadsleyite, respectively) display the pressure-dependent behavior of the most intense group around 900 cm^{-1} showing the general trend of all bands to shift toward higher wavenumbers with increasing pressure. The relative movement of the band group of both samples is similar, but as mentioned before in the case of the hydrous wadsleyite, the bands are less separated from each other. Since the overlapping and broadness of the bands make it difficult to analyze single maximum positions and FWHM by normal fitting procedures, we applied the autocorrelation analysis. The derived autocorrelation plots in Figures 9a (dry) and 9b (hydrous wadsleyite) show the extrapolated effective line widths of the band group at each pressure step ($\Delta corr$ vs. P in GPa). The general trend for both samples is the same—the slope of $\Delta corr$ with increasing pressure is positive but turns negative at some point. The turning point defines the pressure of the discontinuity: it is located around 10.0(7) GPa for the dry and at about 8.4(7) GPa for the hydrous wadsleyite.

All FIR bands are of medium to weak intensity. After the first measurements with the strontium feldspar, we applied some improvements to the microscope (signal intensity, enlargement of the gasket hole), which enhanced the resulting spectra and made the method more sensitive for detecting changes in the FIR range. Figures 10a and 10b show the pressure-dependent spectra of wadsleyite (600–50 cm^{-1}) measured with the FIR-microscope at BESSY. The black marks in Figure 10 highlight the bands, which undergo the most significant changes during pressure increase.

Dry wadsleyite (Fig. 10a). With increasing pressure, the stretching band at 422 cm^{-1} shows an abrupt discontinuity from pressure step 10.3(7) to 11.4(7) GPa. Before, the band shifted slightly to higher wavenumbers, whereas above 11.4(7) GPa it shows strong broadening and flattening until it almost disappears during further pressure increase. In the case of the translational mode T(M) at 361 cm^{-1}, one observes a similar behavior (slight wavenumber shift with increased pressure) until 10.3(7) GPa. The next pressure step leads to the evolution of a new mode at 390 cm^{-1} that exists up to the maximum pressure of 11.6(7) GPa. The rotational band at 260 cm^{-1} is of quite low intensity and keeps its position during pressure increase. At the specific pressure step from 10.3(7) to 11.4(7) GPa its intensity is increased. One should note that the growth in intensity of the band is visible in the spectrum measured at 10.3(7) GPa but becomes more significant as the pressure is increased to 11.4(7) GPa. The band T(M) at 212 cm^{-1} seems to disappear or at least shows extreme broadening in the same pressure region.

Hydrous wadsleyite (Fig. 10b). The modes at 422 and 212 cm^{-1} are only weakly developed or not visible. The translational mode T(M) at 361 cm^{-1} shows—similar to the dry equivalent—a small wavenumber shift up to pressure step 7.7(7) GPa. At 8.9(7) GPa, we suddenly find the evolution of a new band at 389 cm^{-1}. This mode is also stable up to the maximum pressure of 23.7(7) GPa. The hydrous wadsleyite shows another striking behavior: The rotational band at 260 cm^{-1} is very weak and flat-lying and stays constant until 7.7(7) GPa. As pressure is increased to 8.9(7) GPa, it probably splits into two bands combined with a strong increase of intensity that is comparable to the observation in the dry wadsleyite but more pronounced.

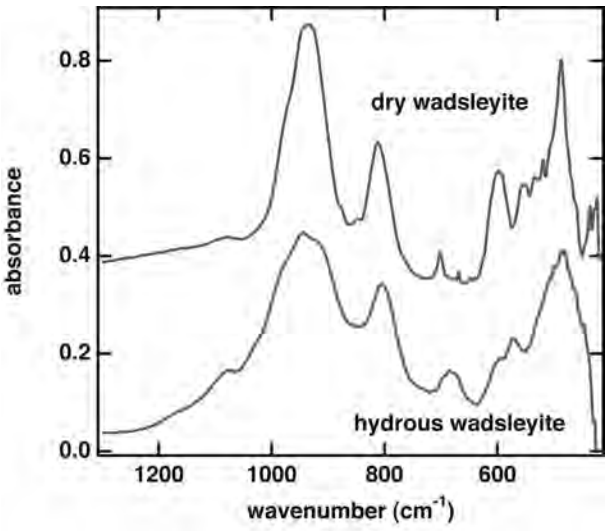

FIGURE 7. Absorption MIR spectra of dry and hydrous wadsleyite. The spectra were taken on thin films of wadsleyite ground with KBr-powder.

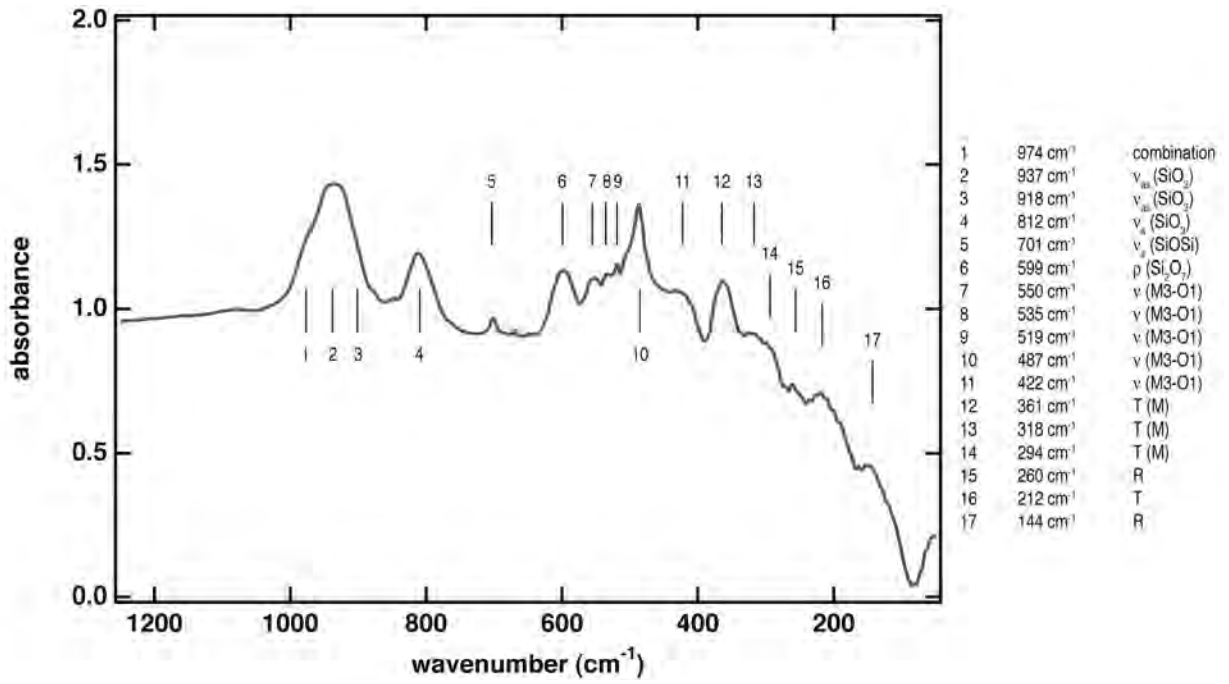

FIGURE 6. Merged absorption spectrum (MIR and FIR) of dry wadsleyite with band assignments after Cynn and Hofmeister (1994).

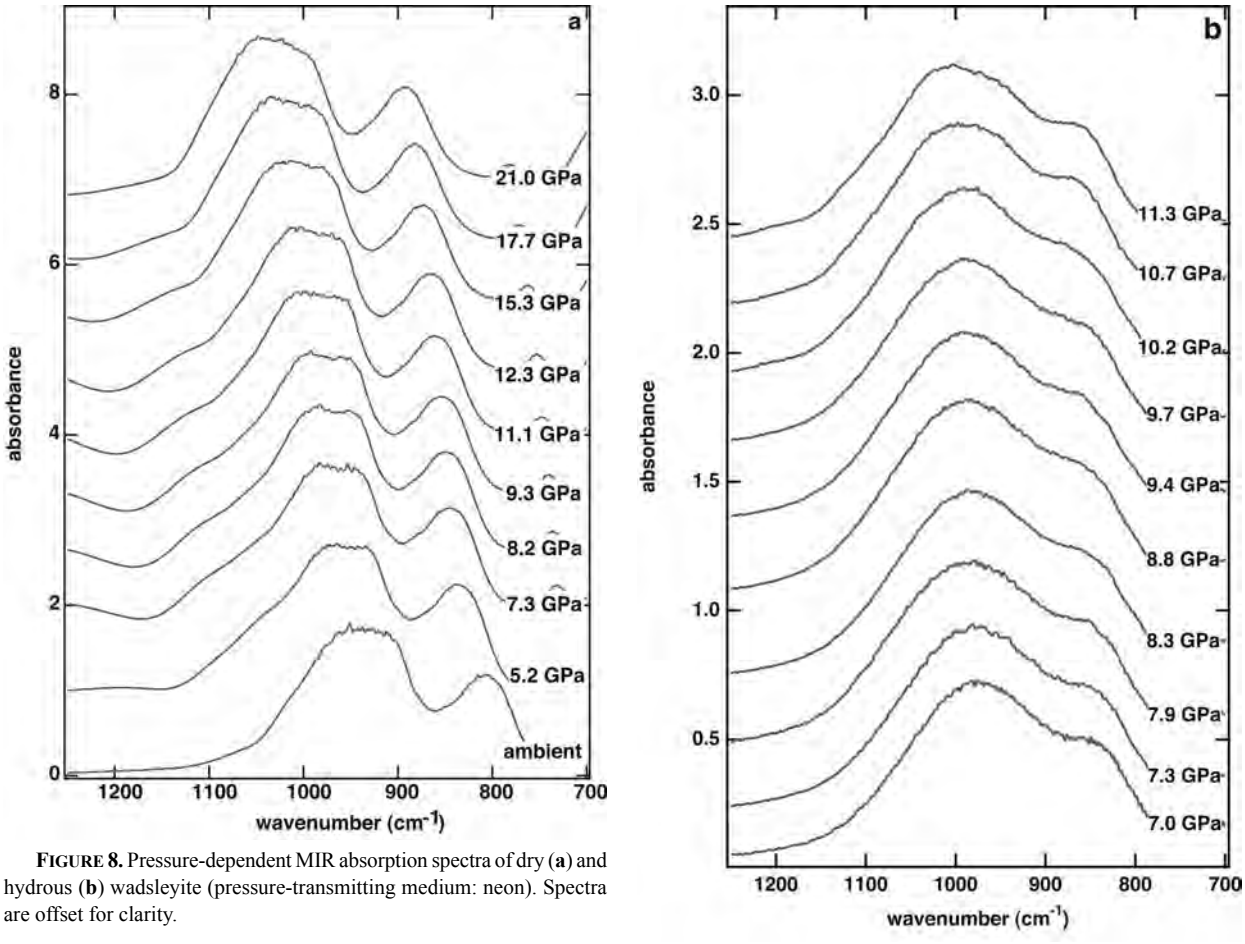

FIGURE 8. Pressure-dependent MIR absorption spectra of dry (**a**) and hydrous (**b**) wadsleyite (pressure-transmitting medium: neon). Spectra are offset for clarity.

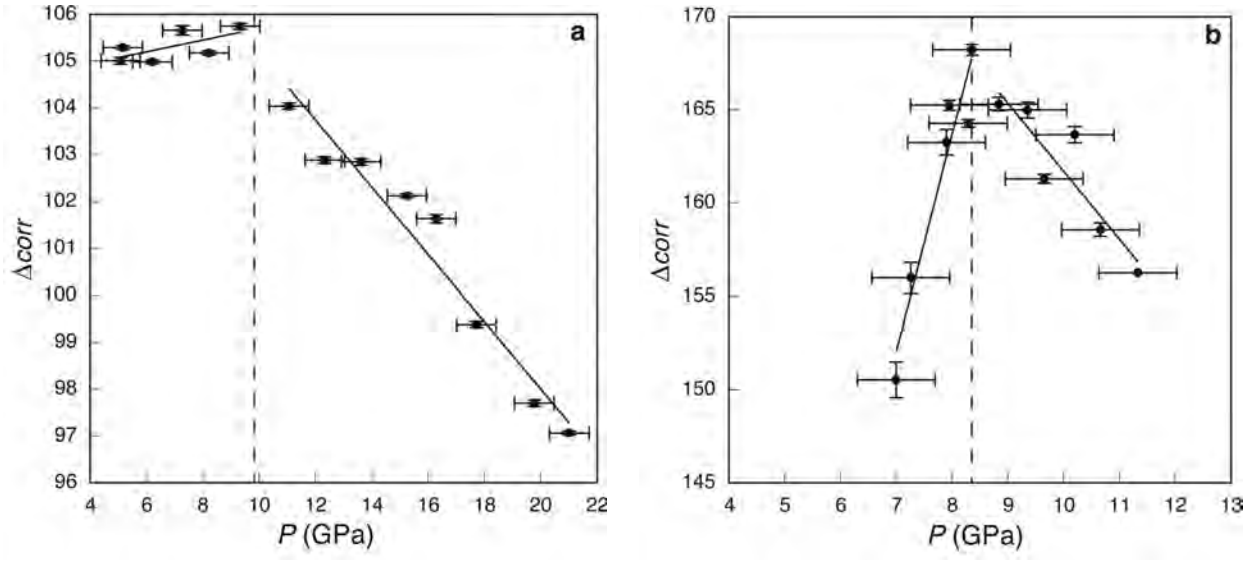

FIGURE 9. Autocorrelation plots of dry (**a**) and hydrous (**b**) wadsleyite. The offset range was defined to 8–30 cm^{-1}. We applied a third-degree polynomial to extrapolate Δ*corr* at *w'* = 0. The black lines represent the trends of slope and their approximate intersections mark the position where the variation of Δ*corr* vs. *P* displays discontinuities (see dashed lines). The plot for the dry wadsleyite (**a**) shows such a discontinuity around 10 GPa. The intersection for hydrous wadsleyite (**b**) lies at about 8.4 GPa. Error bars: *P* = 0.7 GPa; Δ*corr* = 2σ from autocorrelation analysis.

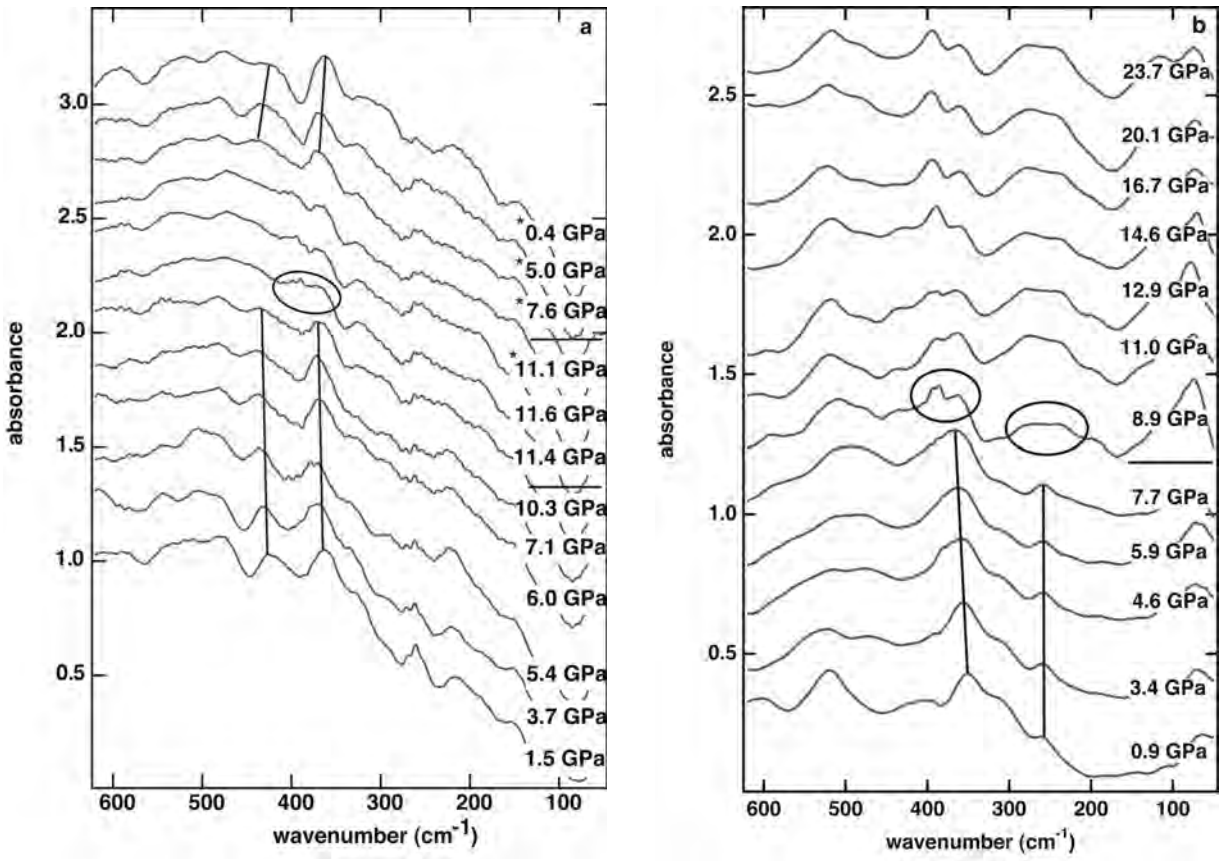

FIGURE 10. Pressure-dependent FIR absorption spectra of dry (**a**) and hydrous (**b**) wadsleyite (pressure-transmitting medium: petroleum jelly). Spectra marked with (*) were measured during decompression. The black lines and circles serve as guide. The horizontal lines mark the significant pressure steps. Spectra are offset for clarity.

In contrast to the series of spectra in the MIR region, an autocorrelation analysis in the FIR was not performed because the analysis requires a linear baseline correction, which was not possible.

DISCUSSION

The mid and far IR spectra of both strontium feldspar and wadsleyite show a pressure-induced shortening of bonds, which is expressed by a band shift toward higher wavenumbers. In addition, the spectra reveal structural changes documented by discontinuities with increasing pressure. Both wadsleyite and strontium feldspar show an increase in the number of bands when passing the respective phase transition, which implies a decrease in symmetry for the high-pressure structure. We performed repeated high-pressure experiments on each sample with all of them yielding consistent and reproducible results (see Table 2). All changes observed during pressure increase were fully reversible under decompression.

In the case of both the strontium feldspar and iron-free wadsleyite analyses, we observed abrupt changes in the infrared spectra as a function of pressure. We found it remarkable that the strontium feldspar displayed the more obvious changes in the MIR region and only slight ones in the longer wavelength range of the FIR, whereas the opposite is true for the wadsleyite. Both minerals consist of $Si(Al)O_4$-structures, which are generally highly resistant to pressure changes. However, the strontium feldspar, as representative for crustal material, had been synthesized at significantly lower pressures than the denser mantle phase wadsleyite. In principle, the pressure response of a more rigid crustal material should differ completely from the behavior of a denser mantle mineral. The structure of strontium feldspar is less close-packed, hence more compressible and therefore displays a more pressure-sensitive behavior in the MIR region where the silicate units have their most intense bands.

Another interesting result of this study is the observation that water incorporation in the mantle mineral wadsleyite changes its pressure-dependent behavior. We observed a shift of a phase transition of about 1.6 GPa to lower pressures in the hydrous wadsleyite compared to the dry one. In contrast, the strontium feldspar shows no displacement of the observed phase transition at 6.5(5) GPa whether water is incorporated in the structure or not. Hydrogen incorporation in mantle minerals softens and widens their structure (e.g., Jacobsen et al. 2005; Smyth et al. 2003). In hydrous wadsleyite, *b* is elongated (see Table 1) and we observe a larger cell volume compared to the dry phase. We therefore argue that water incorporation in denser (mantle) materials such as wadsleyite and enstatite has a stronger influence on the structural behavior compared to less dense minerals, e.g., from the crust.

Strontium feldspar

The strontium feldspar showed evidence of a phase transition at 6.5(5) GPa and another change around 11.0(5) GPa in both IR spectral regions. The evolution of new bands in the MIR can be related to a decrease in the symmetry of the structure. Since this region is characteristic for vibrations of the SiO_4- and AlO_4-tetrahedra, one can assume that a major structural change within these units occurs especially when passing the first discontinuity at 6.5(5) GPa. The behavior of bands in the FIR is less pronounced, but the changes in slope displayed in Figure 4 argue for discontinuities at similar pressures. These observations are in good agreement with a study of Pandolfo et al. (in review). They performed in situ single-crystal X-ray diffraction on hydrous strontium feldspar (hydrous crystals coming from our experiment) and found a phase transition at 6.6 GPa from space group $I2/c$ to $P2_1/c$. Comparable studies on an anhydrous sample clearly showed that the transformation pressure is not dependent on the water incorporated (Pandolfo et al. in review). In the case of pyroxene, a water content of 1300 wt ppm [vs. 1100(100) for strontium feldspar] caused a shift of the phase transition by up to 2 GPa to lower pressures (Jacobsen et al. 2010), indicating that the observed mechanism is also dependent on the crystal structure. Pandolfo et al. (in review) stated that the single Sr site in the original structure splits into two different sites (by still keeping the monoclinic symmetry) in the new configuration. In principle, one would then expect a more obvious change in our FIR spectra (band splitting and/or appearance of new bands), since that is the region where vibrations involving the Sr cations take place. However, all FIR bands are of quite low intensity compared to the MIR ones and are broadened during pressure increase. Possibly these flat and broadened bands cover the evolution of small bands at higher pressure in the spectra.

For the sake of completeness, one should mention that we also performed pressure-dependent IR measurements in the OH-stretching region and found a strong broadening of the band ν_3 (position at ambient conditions: 3629 cm^{-1}) combined with a discontinuity in the wavenumber shift of exactly that band between 8 and 9 GPa. Based on the results of Pandolfo et al. (in review) and our results in the MIR and FIR region, we assume that the broadening of ν_3 is due to the evolution of two bands caused by the initial splitting of the unique Sr site into two different ones. The splitting must start already at lower pressures (6–7 GPa) but is only visible in the spectra at higher pressures.

The discontinuity around 11.0(5) GPa (MIR) is hardly visible in the far IR spectra (only the band at 180 cm^{-1} displays a clear break in slope, the other bands are broadened in a wide range starting at about 11–13 GPa), and beyond that has not yet been proposed. Its nature remains unclear and the changes may also be caused by an ongoing amorphization. In particular, the broadening and smearing of bands around 11.0(5) GPa is an indication of an incipient amorphization process rather than a transformation to another symmetry change.

We observed no significant difference between the spectra by using either CsI or annealed argon as the pressure-transmitting medium.

Wadsleyite

The pressure-dependent spectra of the hydrous and anhydrous wadsleyite display similar discontinuities for the two IR regions, which are fully reversible by decompression. Since the same mechanism of structural change is observed in both samples, we assigned the discontinuities to one type of phase transition occurring at different pressures due to different amounts of hydrogen incorporated in the structures. The dry sample underwent a structural change between 10.3(7) and 11.4(7) GPa, which is marked by the appearance of at least one new infrared active band. The hydrous sample displayed a similar behavior between 7.7(7) and 8.9(7) GPa. Earlier studies found evidence for a second-order structural phase transition in wadsleyite, which are in agreement with our results: Chopelas (1991) conducted a Raman study on pure magnesium wadsleyite (it is not known if water was present) that revealed a structural second-order phase transition at around 9.2 GPa. Cynn and Hofmeister (1994) performed MIR and FIR spectroscopy on a hydrous (0.21 wt% H_2O), iron-bearing sample and confirmed a discontinuous structural change near 10 GPa. They also analyzed pressure-dependent crystallographic data taken from literature on iron-bearing wadsleyite, which support the idea of a phase transition near 9 GPa.

Hydrogen is incorporated into the wadsleyite structure mainly via Mg3 vacancies with protonation of the O1 and O3 oxygen atoms (e.g., Deon et al. 2010a). The higher FWHM of MIR bands in the hydrous phase compared to the dry one may be caused by removal of the degeneracy of the SiO_3 stretching modes due to local disorder. Such an effect has also been observed for ringwoodite (Koch-Müller et al. 2010). A second mechanism leading to a visual broadening of the SiO_3 stretching band group may be the occurrence of additional Mg-O-H bending vibrations. These modes are expected in the MIR with increasing water incorporation and it seems likely that the new band in the hydrous wadsleyite at 682 cm^{-1} overlapping with the symmetric stretching vibration ν(SiOSi) at 701 cm^{-1} (see the comparison of dry and hydrous MIR spectra in Fig. 5) is due to Mg3-O-H bending (e.g., Farmer 1974 and see Gröne and Kapphan 1995 for librational OH modes). The intense band at 599 cm^{-1} (dry sample) that strongly decreases with water incorporation has been assigned by Cynn and Hofmeister (1994) as a deformation band of the disilicate unit. However, Wu and Wentzcovitch (2007) assigned it to vibrations of the Mg1, Mg3, and Si atoms. And, as a matter of fact, the decreasing intensity of the band could be explained by an increasing number of vacant Mg3-octahedra caused by the higher water content. Therefore we follow the assignment of Wu and Wentzcovitch (2007). All hydrated samples (also others not discussed here) display a new band at 573 cm^{-1}. This may be an additional band due to water incorporation (e.g. differentiation between Mg-O1-H1 and Mg-O3-H2) or the dry wadsleyite–band at 550 cm^{-1} is shifted to higher wavenumbers in the hydrous samples. The latter interpretation is more likely since in both studies (Cynn and Hofmeister 1994; Wu and Wentzcovitch 2007) the band is associated with movements of the M3-octahedra: in Cynn and Hofmeister (1994), it is solely assigned to ν(Mg3-O), whereas Wu and Wentzcovitch (2007) revealed that all atoms (Si, Mg1–3) are involved in that vibration but found the strongest displacement for the Mg3 atom. Therefore,

increasing water incorporation could shift the energy of the band since more Mg3-octahedra are vacant. The strong band at 487 cm^{-1} is assigned by Cynn and Hofmeister (1994) to vibrations of Mg3-O, whereas Wu and Wentzcovitch (2007) associated it mostly with Mg2 motions. However, the extreme broadening of the band in the hydrous sample is noteworthy and speaks for the occurrence of additional bands due to hydrogen incorporation. Whereas Cynn and Hofmeister (1994) assigned the band at 422 cm^{-1} as a stretching mode ν(M3-O1), in the density functional study of Wu and Wentzcovitch (2007) it has been classified as being caused mostly by motions of Mg1 and the surrounding oxygen octahedron. However, the pressure-induced broadening of this and other bands in the dry sample possibly represents an incipient amorphization of the structure driven by compression as described by Richet and Gillet (1997). As previously mentioned, we observed a similar behavior in strontium feldspar showing a broadening and smearing of the bands with pressure. By far more obvious is the evolution of a new band at 390 cm^{-1} with pressure increase observable both in the dry and the hydrous wadsleyite. Wu and Wentzcovitch (2007) relate the adjacent band at 361 cm^{-1} to strong displacements of Mg3 and Mg1. Therefore, one can assume that the new band also involves vibrations of one or several Mg octahedra. As the evolution of new bands indicates a decrease of symmetry, the formation of another Mg-site in the wadsleyite-structure seems likely (as this behavior occurs in both the dry and the hydrous sample). The splitting of the band at 260 cm^{-1} accounts for the same argument as it is classified as being caused by motions of Mg2 and Mg3.

In summary, one observes that the most striking changes in the pressure-dependent spectra of both wadsleyite samples involve motions of the Mg atoms, especially at the Mg3 position.

It is known that wadsleyite can change to monoclinic symmetry due to water incorporation. Interestingly, Smyth et al. (1997) reported that in the monoclinic structure (space group *I*2/*m*) the Mg3 position splits into two non-equivalent ones (Mg3a and Mg3b) and the same happens for the O4 position. Accordingly, our observations can be interpreted as pressure-induced structural change of wadsleyite from orthorhombic to monoclinic symmetry that is also dependent on the amount of water incorporation. Whereas wadsleyite, with a high amount of water (up to 3.3 wt% H_2O), can have monoclinic symmetry at ambient conditions, wadsleyite with lower water content (hydrous sample, 12 500 wt ppm H_2O) could display a similar but pressure-driven modification at 8.4(7) GPa. Dry or nearly dry wadsleyite (very little water incorporation in our dry wadsleyite cannot be ruled out) transforms at higher pressures, at around 10.0(7) GPa, into the monoclinic phase. Another possibility that one should take into consideration when thinking of a related phase in the system is wadsleyite II. The hydrous silicate (2.0–2.7 wt% H_2O) also crystallizes as an orthorhombic structure in space group *Imma*. It contains both isolated and bridging oxygen linked SiO_4-tetrahedra (Si_2O_7-groups). It shows similar lattice constants apart from *b*, which is 28.92 Å (about 2.5 times that of wadsleyite) (Smyth and Kawamoto 1997). The properties of wadsleyite II are very close to wadsleyite. Tokár et al. (2010) proposed in a density functional theory (DFT) study that the magnesium end-member wadsleyite II would be stable up to 30 GPa. However, to the best of our knowledge, wadsleyite II has only been found experimentally when containing iron—at least an amount of Fa_{10} (Smyth et al. 1997). As our samples are iron-free, we favor a possible transition to a monoclinic phase over a transformation to wadsleyite II. However, this needs further investigation.

Concluding remarks

We confirm that the measurements with the new FIR/THz microscope were successful and that this method offers a good opportunity to detect and interpret structural changes in good-quality-FIR spectra (e.g., phase transitions) up to high pressures (maximum pressure in this study about 24 GPa, other studies exceeded 30 GPa) and with very small sample volumes (even in powder form).

This method also reveals some advantages compared to the widely used technique of X-ray diffraction for investigating phase transitions with diamond-anvil cells. The indexing of X-ray reflections (especially low-symmetry phases) is more difficult with increasing pressure. This effect is caused by scattering from the diamond and the formation of additional interfering reflections when a transition to a lower-symmetry phase occurs (McGuinn and Redfern 1994).

The results presented herein suggest that the effect of hydrogen incorporation on mineral stability depends not only on the amount of water that is stored but is also mineral specific. It can be dependent on the structural density of the host mineral: the molar volume of strontium feldspar is about 106 cm^3/mol, whereas that of clinoenstatite is ~30 cm^3/mol. It may be that the lower the molar volume of a mineral, the stronger the effect of incorporated defects such as hydrogen on the structure. Thus, further investigations on the effect of stored water in nominally anhydrous minerals (with compositional variations) on phase stabilities are essential.

Acknowledgments

We thank Matthias Gottschalk for providing the Mathematica program for the autocorrelation analysis and Anke Watenphul for her assistance. We are also very grateful for comments and recommendations by L. Dobrzhinetskaya and an anonymous reviewer that greatly improved the manuscript. The work shown here was supported by a grant from Deutsche Forschungsgemeinschaft within the priority program SPP1236 (KO1260/11-1).

References cited

Chiari, G., Calleri, M., Bruno, E., and Ribbe, P.H. (1975) The structure of partially disordered, synthetic strontium feldspar. American Mineralogist, 60, 111–119.

Chopelas, A. (1991) Thermal properties of β-Mg_2SiO_4 at mantle pressures derived from vibrational spectroscopy: implications for the mantle at 400 km depth. Journal of Geophysical Research, B, Solid Earth and Planets, 96, 11817–11829.

Cynn, H. and Hofmeister, A.M. (1994) High-pressure IR spectra of lattice modes and OH vibrations in Fe-bearing wadsleyite. Journal of Geophysical Research, 95, 17717–17727.

Deon, F., Koch-Müller, M., Rhede, D., Gottschalk, M., Wirth, R., and Thomas, S.-M. (2010a) Location and quantification of hydroxyl in wadsleyite: New insights. American Mineralogist, 95, 312–322.

Deon, F., Koch-Müller, M., Rhede, D., and Wirth, R. (2010b) Water and iron effect on the P-T-x coordinates of the 410-km discontinuity in the Earth upper mantle. Contributions to Mineralogy and Petrology, 161, 653–666.

Farmer, V.C. (1974) The Infrared Spectra of Minerals. Mineralogical Society Monograph 4, p. 539. Mineralogical Society, London.

Finger, L.W., Hazen, R.M., Jinmin, Z., Jaidong, K., and Navrotzky, A. (1993) The effect of Fe on the crystal structure of wadsleyite β-$(Mg_{1-x}Fe_x)_2SiO_4$, 0.00 = or <x = or <0.40. Physics and Chemistry of Minerals, 19, 361–368.

Gröne, A. and Kapphan, S. (1995) Combination bands of libration + vibration of OH/OD centres in ABO_3 crystals. Journal of Physics: Condensed Matter, 7, 3051–3061.

Hofmeister, A.M., Xu, J., Mao, H.-K., Bell, P.M., and Hoering, T.C. (1989) Thermodynamics of Fe-Mg olivines at mantle pressures: Mid- and far-infrared

spectroscopy at high pressure. American Mineralogist, 74, 281–306.
Iiishi, K., Tomisaka, T., Kato, T., and Umegakai, Y. (1971) Isomorphous substitution and infrared and far infrared spectra of the feldspar group. Neues Jahrbuch für Mineralogie Abhandlungen, 115, 98–119.
Inoue, T., Yurimoto, H., and Kudoh, Y. (1995) Hydrous modified spinel, $Mg_{1.75}SiH_{0.5}O_4$: a new water reservoir in the mantle transition region. Geophysical Research Letters, 22, 117–120.
Jacobsen, S.D., Demouchy, S., Frost, D.J., Boffa, B.T., and Kung, J. (2005) A systematic study of OH in hydrous wadsleyite from polarized FTIR spectroscopy and single-crystal X-ray diffraction; oxygen sites for hydrogen storage in Earth's interior. American Mineralogist, 90, 61–70.
Jacobsen, S.D., Liu, Z., Boffa Ballaran, T., Littlefield, E.D., Ehm, L., and Hemley, R.J. (2010) Effect of H_2O on upper mantle phase transitions in $MgSiO_3$: Is the depth of the seismic X-discontinuity an indicator of mantle water content? Physics of the Earth and Planetary Interiors, 183, 234–244.
Koch-Müller, M., Rhede, D., Schulz, R., and Wirth, R. (2009) Breakdown of hydrous ringwoodite to pyroxene and spinelloid at high P and T and oxidizing conditions. Physics and Chemistry of Minerals, 36, 329–341.
Koch-Müller, M., Speziale, S., Deon, F., Mrosko, M. and Schade, U. (2011) Stress-induced proton disorder in hydrous ringwoodite. Physics and Chemistry of Minerals, 38, 65–73 p.
Larson, A.C. and Von Dreele, R.B. (2000) Generalized Structure Analysis System (GSAS). Los Alamos National Laboratory Report LAUR 86-748.
Mao, H.K., Xu, J., and Bell, P.M. (1986) Calibration of the Ruby pressure gauge to 800 kbar under quasi-hydrostatic conditions. Journal of Geophysical Research, 91, 4673–4676.
McGuinn, M.D. and Redfern, S.A.T. (1994) Ferroelastic phase transition along the join $CaAl_2Si_2O_8$-$SrAl_2Si_2O_8$. American Mineralogist, 79, 24–30.
Mrosko, M., Koch-Müller, M., Hartmann, K., Wirth, R., and Dörsam, G. (2010) Location and quantification of hydrogen in Ca- and Sr-anorthite. European Journal of Mineralogy, 22, 103–112.
Neri, F., Saitta, G., and Chiofalo, S. (1987) A simple procedure to remove the interference fringes from optical spectra. Journal of Physics E: Scientific Instruments, 20, 894–896.
Peatman, W.B. and Schade, U. (2001) A brilliant infrared light source at BESSY. Review of Scientific Instruments, 72, 1620–1625.
Richet, P. and Gillet, P. (1997) Pressure-induced amorphization of minerals: a review. European Journal of Mineralogy, 9, 907–933.
Salje, E.K.H., Carpenter, M.A., Malcherek, T., and Boffa Ballaran, T. (2000) Autocorrelation analysis of infrared spectra from minerals. European Journal of Mineralogy, 12, 503–519.
Schmidt, M.W. and Ulmer, P. (2004) A rocking multianvil; elimination of chemical segregation in fluid-saturated high-pressure experiments. Geochimica et Cosmochimica Acta, 68, 1889–1899.
Smyth, J.R., Holl, C.M., Frost, D.J., Jacobsen, S.D., Langenhorst, F., and McCammon, C.A. (2003) Structural systematics of hydrous ringwoodite and water in Earth's interior. American Mineralogist, 88, 1402–1407.
Smyth, J.R. and Kawamoto, T. (1997) Wadsleyite II; a new high pressure hydrous phase in the peridotite-H_2O system. Earth and Planetary Science Letters, 146, E9–E16.
Smyth, J.R., Kawamoto, T., Jacobsen, S.D., Swope, R.J., Hervig, R.L., and Holloway, J.R. (1997) Crystal structure of monoclinic hydrous wadsleyite [β-$(Mg,Fe)_2SiO_4$]. American Mineralogist, 82, 270–275.
Thomas, S.-M., Koch-Müller, M., Reichart, P., Rhede, D., Thomas, R., Wirth, R., and Matsyuk, S. (2009) IR calibrations for water determination in olivine, r-GeO_2 and SiO_2 polymorphs. Physics and Chemistry of Minerals, 36, 489–509.
Thomas, S.-M., Thomas, R., Davidson, P., Reichart, P., Koch-Müller, M., Dollinger, G., Henderson, G.S., and Neuville, D.R. (2008) Application of Raman spectroscopy to quantify trace water concentrations in glasses and garnets. American Mineralogist, 93, 1550–1557.
Tokár, K., Jochym, P.T., Parlinski, K., Lazewski, J., Piekarz, P., and Sternik, M. (2010) DFT study of structure stability and elasticity of wadsleyite II. Journal of Physics: Condensed Matter, 22, 145402.
Tsuchiya, J. and Tsuchiya, T. (2009) First-principles investigation of the structural and elastic properties of hydrous wadleyite under pressure. Journal of Geophysical Research, 114, B02206.
Walker, D. (1991) Lubrication, gasketing, and precision in multianvil experiments. American Mineralogist, 76, 1092–1100.
Wittlinger, J., Fischer, R., Werner, S., Schneider, J., and Schulz, H. (1997) High-Pressure Study of h.c.p.-Argon. Acta Crystallographica, B53, 745–749.
Wu, Z. and Wentzcovitch, R.M. (2007) Vibrational and thermodynamic properties of wadsleyite; a density functional study. Journal of Geophysical Research, 112, B12202.

Manuscript received October 26, 2010
Manuscript accepted July 1, 2011
Manuscript handled by Lars Ehm